Journal of Sustainable Metallurgy (2023) 9:249–265
https://doi.org/10.1007/s40831-022-00642-5

RESEARCH ARTICLE

A Feasibility Study to Minimize the Carbon Footprint of Cast Iron Production While Maintaining the Technical Requirements

Ali Abdelshafy[1] · Daniel Franzen[2] · Amelie Mohaupt[2] · Johannes Schüssler[2] · Andreas Bührig-Polaczek[2] · Grit Walther[1]

Received: 9 March 2022 / Accepted: 12 December 2022 / Published online: 28 December 2022

Abstract

The industrial sector is responsible for significant amounts of CO_2 emissions. Although research activities have already given their attention to major industries such as steel, small sectors such as metal casting have been overlooked. Therefore, there are evident knowledge gaps regarding the environmental impact of the foundry industry and the possibilities of decarbonizing the sector. Herein, this study focuses on the CO_2 emissions associated with cast iron production and introduces an interdisciplinary framework in order to study the environmental impact, technical performance and production costs. The theoretical and experimental analyses illustrate the interconnections between the environmental, technical and economic aspects of cast iron production. The results emphasize the role of the smelting process and renewable energies in decreasing the carbon footprint. In terms of the input materials, the outcomes demonstrate that increasing the steel scrap content achieves considerable reductions in the CO_2 emissions. An alloy composition with a steel scrap content of 25% leads to a minimum carbon footprint of 650 kg CO_2 eq./ton. However, increasing the steel scrap content further results in higher carbon footprints due to the additional materials required to maintain the alloy composition. Moreover, a higher strength and lower ductility of the alloy were recorded due to higher amounts of carbide stabilizing elements. The study highlights the importance of adopting a holistic approach in order to define the optimal material combinations. Hence, the presented interdisciplinary approach can be applied by the foundries in order to achieving the technical, economic and ecological goals of the sector.

The contributing editor for this article was Christina Meskers.

✉ Ali Abdelshafy
ali.abdelshafy@om.rwth-aachen.de

[1] Chair of Operations Management of RWTH Aachen University, Kackertstraße 7, 52072 Aachen, Germany

[2] Foundry Institute of RWTH Aachen University, Intzestraße 5, 52072 Aachen, Germany

Graphical Abstract

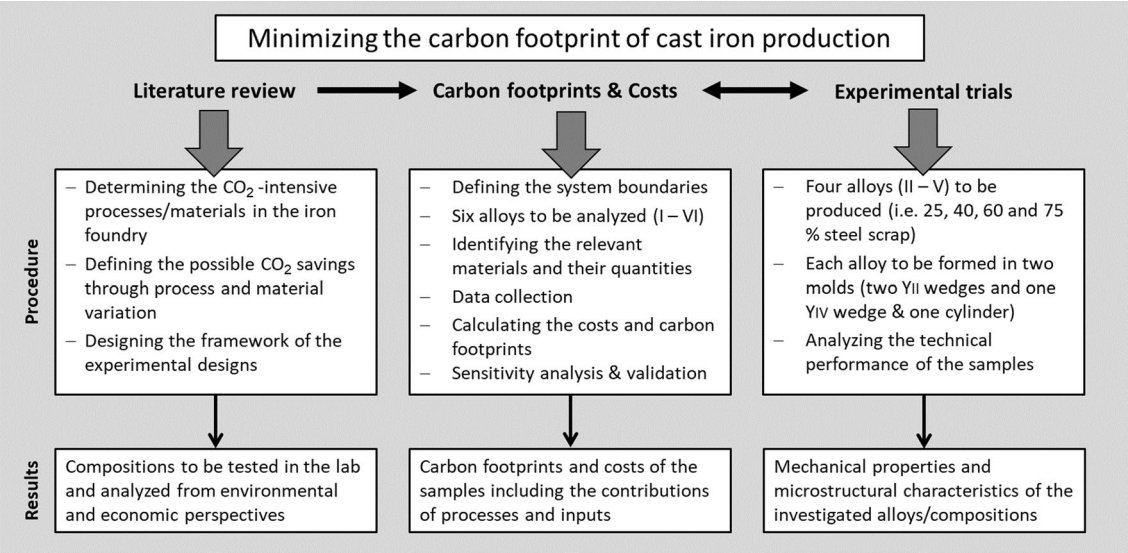

Keywords Energy transition · Carbon footprint · Cast iron · Interdisciplinary assessment · Circular economy · Steel scrap

Introduction

Climate change has enforced the major industrial economies to set environmental goals to mitigate their greenhouse gas (GHG) emissions. For example, the EU has committed to become carbon–neutral by 2050 and Germany wants to achieve this goal even earlier (i.e. 2045) [1]. Herein, the industrial sector has major responsibilities due to the significant amounts of CO_2 emitted by the different industries. The German industries are responsible for 23% of the total annual GHG emissions in Germany due to its process and energy-related emissions, in addition to the indirect emissions related to power consumption [2]. The casting industry is classified as an energy-intensive sector, which means that it also has to deal more intensively with the topic of CO_2 savings. In Germany, metal casting consumes significant amounts of energy such as natural gas, coke and electricity, in addition to the emissions embedded in the inputs such as pig iron. Energy transition incurs both opportunities and challenges for the foundry industry. On the one hand, the industry is the main provider of crucial components for the sector of renewable energies such as cast gears, shafts and hubs for the wind turbines [3, 4]. On the other hand, decarbonizing the sector is associated with various challenges due to its characteristics like small-scale plants and many products and processes.

In a few words, metal casting refers to shaping the respective metal via melting and molding [5]. Depending on the application and required properties, several alloys can be used such as cast iron, steel, aluminum, etc. The sector yields several sophisticated products and intricate designs, some of which are key inputs for other high-value products such as wind energy parts, automotive, and machines. There are approximately 600 foundries in Germany, which secure 70.000 jobs and achieve a turnover of 12.5 billion EUR [6, 7]. In total, the German foundry industry produces more than 5 Mt cast metals, 75% of which are cast iron products [8]. Cast iron alloys are commonly classified into lamellar graphite cast iron (LGI), compacted graphite cast iron (CGI) and spheroidal graphite cast iron (SGI) [9]. For the melting process, various furnaces are currently adopted by the producers such as cupola and induction furnaces.

So far, the production technique has been based on the product's specifications and associated costs. However, reducing the carbon footprint necessitates a new factor, which is the direct and embedded emissions. Although the foundry industry is typically known as environmentally-friendly sector as scrap metals are the main input material [10], this notion is intrinsically not fully correct as the current production processes consume significant amounts of fossil fuels or electricity produced via fossil energy. Moreover, the industry consumes various input materials such as pig iron and inoculants, which have significant amounts of embedded emissions. While there is an extensive number of studies investigating the different technical aspects of the cast iron production, there is an obvious lack of research addressing the environmental impacts.

The analysis of [11] is one of the few studies addressed the topic. The authors compared between the carbon footprint of three materials used in the automotive industry (i.e. thin-wall ductile cast iron, conventional cast iron and cast aluminum), while considering the whole life cycle. Herein, the authors used a parametric model to calculate the associated emissions based on the masses and consumed energy, including the use phase. The study of [12] also aimed at comparing between two materials (i.e. cast iron and aluminum) by considering all the material and energy flows along the life cycle (a cradle-to-grave approach). Similarly, the analyses of [13–15] compared between the environmental impacts of cast iron and other materials such as aluminum, steel, plastics and concrete. However, as can be deduced, these studies do not address the production process of cast iron itself and how the carbon footprint can be minimized. Other studies such as [16, 17] presented more detailed environmental analyses regarding the impacts of casting and molding processes. Nonetheless, they do not indicate practical measures or alternative possibilities to mitigate the CO_2 emissions.

In the few studies that addressed the topic, there is an agreement regarding the crucial role of energy consumption in minimizing the carbon footprint. However, in addition to energy-efficient melting and the switch to renewable energies, there is a great potential to mitigate the CO_2 emissions via the input materials. According to our best knowledge, no study has addressed this topic despite its importance in minimizing the carbon footprint of cast iron products. A recent study of [18] highlighted the significance of the theme, however, the analysis focused on zinc and also did not integrate a technical assessment. A standard cast iron alloy usually contains up to 20% pig iron which is associated with high GHG emissions during the production process (1.45 t CO_2 eq./t pig iron in a modern blast furnace [19]). One way to reduce these emissions is to use a higher amount of steel scrap during the production process. Hence, the aim of this research is to present comprehensive analyses regarding the possibility of minimizing the environmental impact of the cast iron products via using more secondary inputs (i.e. steel scrap).

Herein, the study focuses on the production of ductile cast iron, which is also referred to as spheroidal graphite cast iron (SGI). According to the European standard for ductile iron alloys, DIN EN 1563, it can be classified into the conventional ferritic-pearlitic grades [20]. Due to the comparatively low notch effect of the nodular graphite precipitates, it can show elongations of 22% at fracture with an ultimate tensile strength (UTS) of 350 Mpa. Depending on the pearlite content set, strengths of up to 900 Mpa can likewise be achieved with still 2% elongation at fracture. While the fully ferritic grades are very ductile materials due to a high elongation at fracture, pearlitic grades have increasingly higher strength and are wear resistant. The combination of ductility, strength and good castability allows ductile iron to be widely used material in mechanical engineering, power engineering and the automotive industry [4, 21, 22]. In terms of melting technology, cupola or medium frequency induction furnaces are usually used. While cupola furnace depends on fossil fuels, the induction furnace is supplied with electric energy [23].

In order to evaluate the process route of cast iron holistically, it is necessary to evaluate both the metallurgical and technological criteria. In particular, microstructural aspects as well as mechanical properties have to be still achieved to ensure a continued competitiveness of cast iron alloys and further enable technical applications. Hence, the ecological analysis is accompanied with experimental casting trials to produce the respective samples and perform the required tests to examine their microstructural and mechanical properties. Moreover, a cost analysis has been conducted in order to explore the impact on the production expenses. In the following section, the methodological framework of the techno-economic and environmental (TEE) assessment is first explained and the investigated material and samples are presented. Thereafter, the results and outcomes are discussed in "Results and Discussion". Finally, "Conclusions and Outlook" presents the main conclusions and outlook for future research.

Methdology and Materials

In order to develop a suitable methodological approach, the relevant studies on similar problems have been reviewed. Promoting sustainability in the industrial sector necessitates developing integrative methods in order to realize the required interdisciplinarity. This is particularly indispensable if the technical, economic and environmental performances can be influenced by the introduced measures simultaneously. While Life Cycle Assessment (LCA) or carbon footprint can assess the direct and indirect environmental impact of the available alternatives, an interdisciplinary evaluation approach is required to investigate if the economic and technical performances are competing with the environmental measures (i.e. in the sense of a trade-off).

Therefore, TEE assessments have been used in various studies addressing similar questions. For example, the sensitivity analyses of [11] investigated the impact of different steel scrap and pig iron ratios on the carbon footprint. Herein, the study assumed that that these changes will only influence the environmental impact of the different cases. However, such assumption overly simplifies the situation as the such variations are also associated with changes in the metallurgical properties, which necessitate technical analyses. According to our best knowledge, no studies in the literature have yet adopted an evident integrative approach

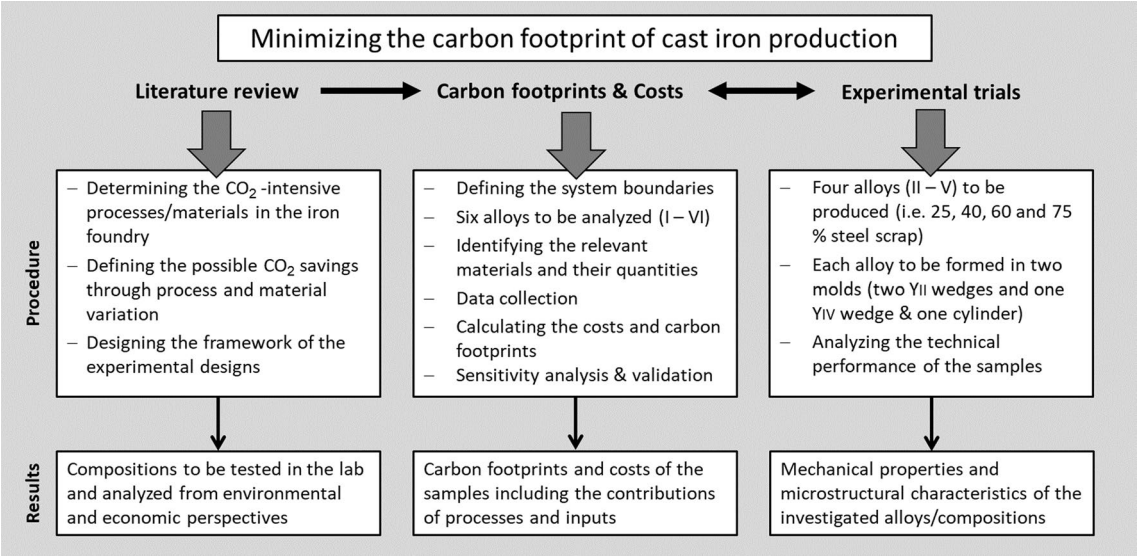

Fig. 1 Study's framework

to address sustainability in the field of casting production. Nonetheless, relevant approaches have been developed by studies addressing material recycling in other industries. For example, the recent studies of [24, 25] assess the recovery processes of alumina from aluminum dross from the economic and environmental perspectives, while [26–29] conducted various TEE assessments on plastic recycling.

Methodologically, these studies implement scenario analysis by means of assessing the techno-economic and environmental performance of different systems or applications. Herein, LCA or carbon footprint are used to evaluate the environmental impact and the associated costs are quantified to assess the techno-economic performance. Accordingly, the optimum system or option can be selected via comparing the investigated scenarios. However, the technical assessment is usually omitted from these analyses, and the techno-economic assessment focuses mainly on the costs. Thus, these approaches usually assume that the technical performance or the final outputs are similar with regards to material properties and quality. For example, it is assumed that the recycled plastic will have the same functions and properties regardless of the recycling process. Although such assumptions can be accepted for some materials, they cannot be applied to cast products. Therefore, this study follows the same approach via implementing TEE assessments, but also considers the technical aspects via examining the mechanical properties and microstructural characteristics of the relevant samples.

As shown in the study's framework (Fig. 1), the research procedure can be divided into three parts. Firstly, a literature research was conducted in order to define the CO_2-intensive processes, materials and mitigation potentials in the cast iron production. In order to study the possibility of minimizing the carbon footprint via the material inputs (i.e. steel scrap and pig iron), six different alloys, referred to as alloy I–VI, were defined in order to be investigated. Alloy I contains 15.2 wt% pig iron and no scrap steel, which serves as the reference alloy. Alloys II–V contain 25, 40, 60 and 75 wt% of steel scrap, respectively, with no pig iron addition. To study the effect of the amount of steel scrap, these alloys were studied experimentally in casting trials and subsequent analyses. 75 wt% of steel scrap was chosen as the maximum amount, as steel scrap fraction of up to 80% are used in industrial environment. Alloy VI can be regarded as a "mixed" alloy composed of equal shares of pig iron and steel scrap (8 wt% each).

Herein, the required additives (e.g. carburizing agent, ferrosilicon FeSi75, etc.) have been added to the samples to be eventually comparable to the composition of the reference alloy EN-GJS-400-15 according to DIN EN 1563 (C = 3.5 wt%, Si = 2.5 wt%, Mn < 0.2 wt%, P < 0.03 wt%, S < 0.02 wt%, Mg = 0.04 wt%). The detailed charging composition of all investigated alloys is depicted in Fig. 2. After defining the system boundaries and collecting the required economic and environmental inventories, the carbon footprints and the relevant costs of the different compositions are then calculated. Simultaneously, a series of four experimental tests was carried out in order to analyze the effect of increasing steel scrap content of the respective samples.

Environmetal and Economic Assessments

The environmental assessment (i.e. carbon footprint) has been conducted in accordance with ISO 14067 [30].

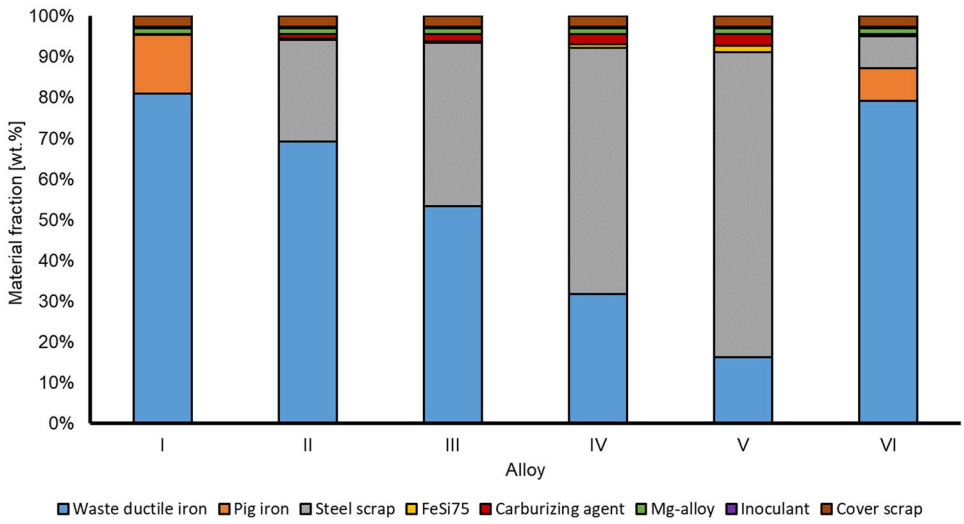

Fig. 2 Calculated charging compositions of the investigated alloys

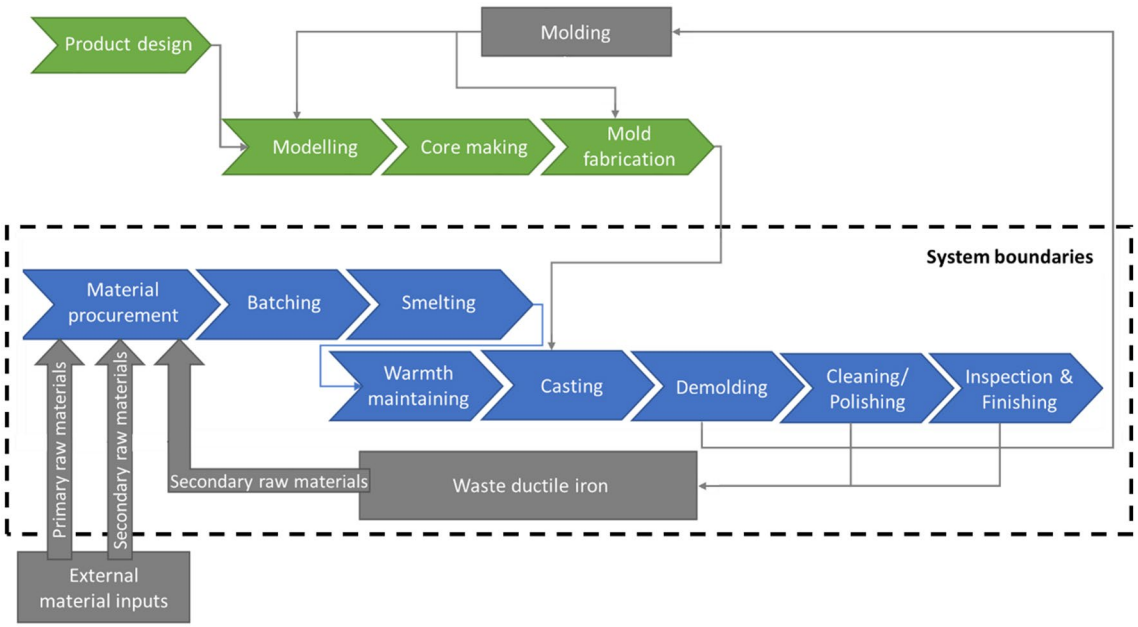

Fig. 3 Overview of the cast iron production and system boundaries

Herein, the analysis is classified into four phases (i.e. goal and scope definition, inventory analysis, impact assessment and interpretation). In terms of goal and scope (i.e. first phase), the study investigates the possibility of minimizing the environmental impact of the cast iron products via using more secondary inputs (i.e. steel scrap). Hence, the scope and boundaries of the analyses are the input materials and the processes of charging and smelting. As shown in system boundaries (Fig. 3), the study does not take into account all upstream and downstream processes that are not impacted by the charging composition, such as mold fabrication. Also, the treatment of the kiln exhaust gases was discarded as its environmental impact doesn't influence the analyses. As the main study's objective is to investigate the different charging compositions and the effect of increasing steel scrap content on the microstructure and mechanical performance, one ton of liquid cast iron that fulfills the specifications of EN-GJS-400-15 was selected as a functional unit. This unit ensures an intuitive understanding of the result variables and good comparability with the results of other studies either on cast iron or other metallic alloys such as [11, 15]. The same system boundaries, inputs and functional unit have been also used to derive the production cost of each alloy.

Table 1 Life cycle inventories of the investigated alloys

Alloy	Electricity	Waste ductile iron	Pig iron	Steel scrap	FeSi75	Carburizing agent	Mg-alloy	Inoculant	Cover scrap
	kWh	kg							
I	650	810.6	145.9	0	0.811	0.486	14.368	3.352	26.34
II	650	693.9	0	250.4	3.017	10.559	14.368	3.352	26.34
III	650	535.1	0	401.34	4.459	16.95	14.368	3.352	26.34
IV	650	318.4	0	605	10.19	24.2	14.368	3.352	26.34
V	650	162.9	0	749.6	16.29	29	14.368	3.352	26.34
VI	650	794.2	79.42	79.42	1.59	3.12	14.368	3.352	26.34

Table 2 Carbon footprints and prices of the input materials [31–34, 46]

Input	Emission factor	Unit	Reference	Price	Unit	Reference
Electricity	733	Kg CO_2 eq./MW	[31]	96.85	EUR/MWh	[46]
Pig iron	1.7	t CO_2 eq./t		640	EUR/t	Values from a regional foundry [47]
Ferrosilicon 75% Si	4.0	t CO_2 eq./t	[33]	1,850	EUR/t	
Inoculant	14.5	t CO_2 eq./t	[32]	2,750	EUR/t	
Mg-alloy	5.0	t CO_2 eq./t	[33, 34]	2,762	EUR/t	
Carburizing agent	3.5	t CO_2 eq./t	[32]	590	EUR/t	
Steel scrap	0	t CO_2 eq./t	[36, 37]	300	EUR/t	
Cover scrap	0	t CO_2 eq./t		300	EUR/t	
Waste ductile iron	0	t CO_2 eq./t		152	EUR/t	
Transport (land)	0.16	kg CO_2 eq./ton.km	[31]	Included in the final prices		
Transport (sea)	0.02	kg CO_2 eq./ton.nautical mile				

Table 3 Distance between the manufacturers and the location of analyses

Element	Distance (km)
Steel scrap	6
Ferrosilicon 75%	680
Mg-alloy	650
Inoculant	50
Carburizing agent	100

Table 4 Transportation data of pig iron

Transportation	Distance
Transportation to the port of Rio de Janeiro	430 km
Shipping to the port of Rotterdam	5138 nautical miles
Transportation to NRW	260 km

The life cycle inventories, relevant emissions factors and prices (Tables 1 and 2) are collected for the second phase (i.e. inventory analysis). As the emission factors of some materials were not found in the Ecoinvent database (version 3.5) [31], their values have been adopted based on [32–34]. The carbon emissions associated with transportation are based on the distance between the materials' manufacturers and the location of analyses (i.e. NRW). As all alloying elements (except pig iron) are produced in Germany, it is assumed that they have been transported via trucks. For pig iron, different transportation modes were used as it is produced outside Germany (i.e. Brazil). The value of estimated distances are indicated in Tables 3 and 4. In terms of energy, the required amount to melt one ton of cast iron is normally in the range of 500–1000 kWh, depending on the carbon content [35]. Herein, a survey was conducted to ask some regional producers about their specific energy consumption, which results in a lower range (i.e. 450–750 kWh/ton). Hence, an average value of 650 kWh/ton was considered for the analyses.

The steel scrap and waste ductile iron are considered end-of-life flows and thus their carbon footprint is assumed as zero. It should be noted that the allocation of the environmental impact is a controversial topic in the environmental assessments while addressing waste streams and by-products. For example, if the environmental impact should be allocated based on the mass or the monetary value. The studies of [36, 37] explain numerous allocation methods and show their significant impact on the outcomes. Also,

Table 5 Chemical composition of the low-alloyed steel scrap (in wt%)

Steel	C	Si	Mn	P	S	Mg	Cu	Al	Fe	Cover scrap for alloy
No. 1	0.070	0.19	0.48	0.013	0.007	0.0002	0.175	0.004	Bal.	II, V
No. 2	0.018	0.01	0.18	0.016	0.006	0.0002	0.021	0.041	Bal.	III, IV

the studies of [38–41] address the theme of metal recycling and suitable methods to determine the environmental impact associated with the produced metals and scrap. According to [42, 43], there is no one right allocation method and the analysts normally have flexibility while modelling. As there is no clear agreement on one superior approach, this study adopts a cutoff approach, via which the carbon footprint is calculated within the defined system boundaries. Therefore, the environmental impact is allocated to the primary production and no environmental burdens are allocated to the waste streams. This approach has already been used by other studies such as [44], which considered a zero carbon footprint for the steel scrap used in the steel production process.

For the third phase (i.e. impact assessment), the calculations have been implemented via OpenLCA software (version 1.10.3) using the collected life cycle inventories [45]. As study focuses on the carbon footprint, the impact category of global worming potential (GWP100) was selected and (CML-IA baseline) was used as a life cycle impact assessment (LCIA) method. The last phase (i.e. interpretation) is discussed in the following section (results and discussion) along with the economic and technical assessments. For the economic assessment, the prices of material inputs have been retrieved based on the purchasing prices of a German foundry located in North Rhine-Westphalia (NRW).

Technical Assessment

To conduct the experimental tests, 250 kg of casting batches of alloys II–V were produced based on waste ductile iron (EN-GJS-400-15), ferrosilicon (FeSi75), steel scrap and a carburizing agent. The steel scrap used is a low-alloy stamping scrap from a profile stamping machine. The chemical compositions of this consumed steel scrap (steel No. 1) is illustrated in Table 5. For melting of the alloys, a 250 kg medium-frequency induction furnace from *Otto Junker* was used. The ingot materials were heated and melted to 1520 °C. This temperature was held for approximately 5 min in order to remove the impurities from the melt. Subsequently, 1.3 wt% of Mg pre-alloy (VL 63O) was placed onto the bottom of a treatment and pouring ladle. At 1520 °C the melt was poured into the treatment ladle for conducting the magnesium treatment. By adding magnesium to the melt, a nodular graphite morphology is obtained in the as-cast microstructure. After deslagging the melt surface, 0.35 wt% of cerium-containing inoculant SMW 605 is stirred into the melt just before pouring in order to ensure stable solidification of carbon. Cerium acts as a graphite nucleating agent in the inoculant and favors graphite precipitation during solidification of the alloy. Due to the availability, the cover scrap used for alloys II and V was steel No.1, and No.2 for alloys III and IV, according to Table 5.

After the Mg treatment and inoculation, the melt was poured at approximately 1380 °C. For each alloy, two of the casting geometries indicated in Fig. 4 was produced, which consisted of two Y_{II} standard test blocks, one Y_{IV} standard test block according to DIN EN 1563 and one additional insulated cylinder [48, 49]. Therefore, the casting blocks are represented with a thermal modulus of 0.96 cm (Y_{II}), 1.74 cm (Y_{IV}) and 3.29 cm (cylinder) serving as an indicator for the solidification time. The corresponding cooling curves and solidification times are given in Fig. 5. For each casting geometry one metallographic specimen of each test block was machined for metallographic analyses. Additionally, one tensile test specimen out of Y_{II}- and two tensile test specimens were machined out of both Y_{IV}- and cylinder geometries, respectively. The tensile specimens are taken from the test blocks according to the positions marked in red in

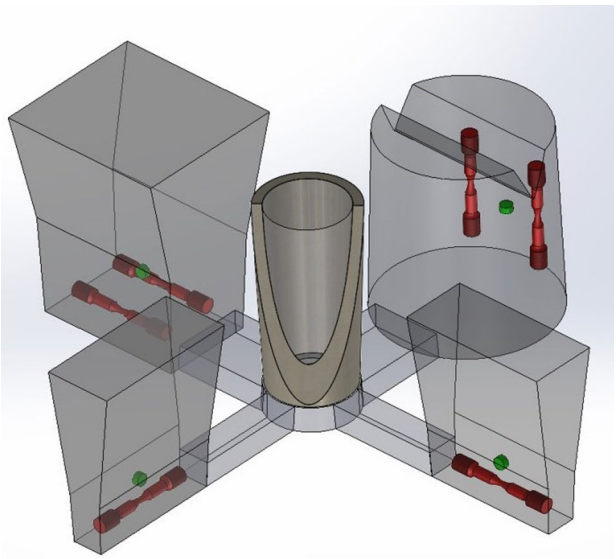

Fig. 4 Casting geometry for the casting trials (red: tensile test specimen with a length of 110 mm; green: metallographic specimen) (Color figure online)

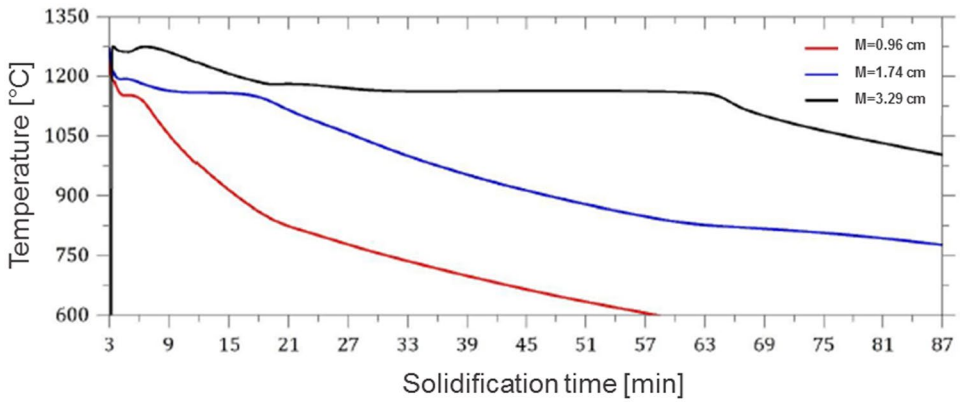

Fig. 5 Representative cooling curves for specimen locations in the casting geometries that were produced according to [52] (*M* values are the thermal modulus of the specimen)

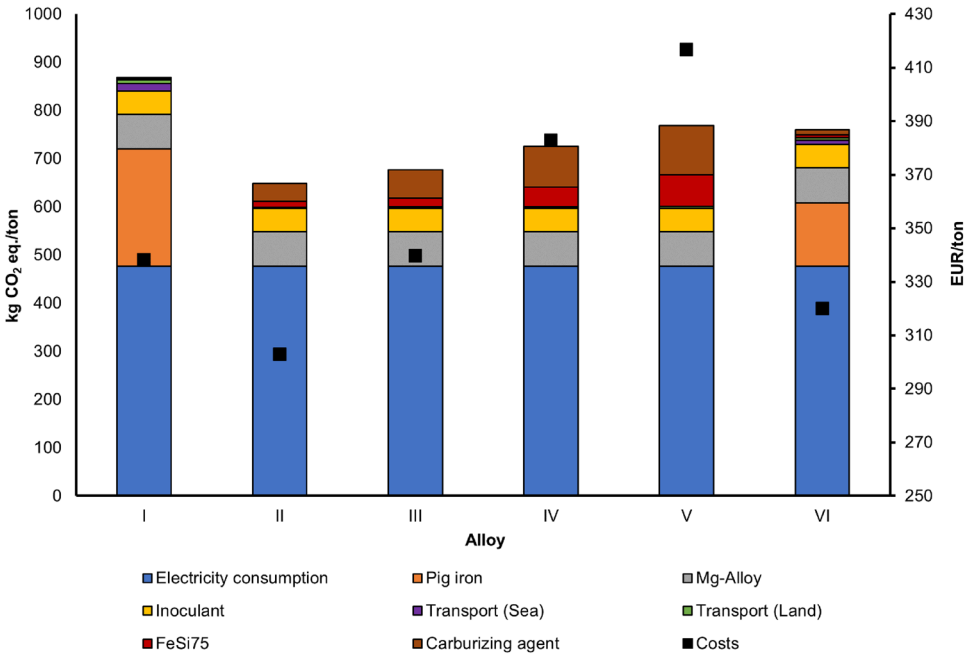

Fig. 6 The carbon footprint and costs of the relevant inputs

Fig. 4 by using a water-cooled core drill. The specimens are then machined according to DIN EN 1563 by turning them to the dimensions shown in Fig. 4 and a length of 110 mm. The quasi-static tensile tests are then carried out according to EN ISO 6892-1 [50].

The specimens marked in green in Fig. 4 are used as metallographic specimens. The specimens are ground stepwise with silicon carbide grinding paper and then polished with a diamond suspension. Following the preparation steps, a digital image analysis is performed. Graphite analysis is used for this purpose and is carried out in accordance with DIN EN ISO 945-4 standard [51]. For this purpose, five images are taken of each specimen at ×100 magnification with a resolution of 2600×2600 pixels. Subsequently, the images are characterized using ImageJ image analysis software. To be considered as graphite particles, there must be a minimum graphite particle area of 25 µm. A detailed qualitative evaluation of the adjusted microstructure is carried out by taking pictures of the cast specimens in the Nital-etched state using a Nital-solution consisting of 3% HNO_3 and 97% alcohol (C_2H_5OH). Immediately after etching, five images are taken of each sample under the light microscope at ×100 magnification. Following the image acquisition, the pearlite content is also quantified using the ImageJ software.

Results and Discussion

Carbon Footprint and Costs

The carbon footprint and the relevant costs of the investigated samples are depicted in Fig. 6. The carbon footprint of alloy I is the highest (868.5 kg CO_2 eq./ton), of which more than 50% is attributed to the energy required for melting

and approximately 30% is the embedded emissions of the pig iron input (i.e. 145.9 kg CO_2 eq.). Contrariwise, adding 25 wt% steel scrap (i.e. alloy II) results in the lowest carbon footprint (lower than 650 kg CO_2 eq./ton). Such significant reduction can be attributed mainly to abandoning the pig iron. Increasing the steel scrap content to 40% in alloy III has caused a minor retreat in the emissions savings, as the carbon footprint has reached 677 kg CO_2 eq./ton. By adding low-alloyed steel scrap, the silicon and carbon content of a cast iron alloy decreases considerably. To compensate for this deficit, corresponding carbon and silicon-containing materials must be added to the alloy (i.e. carburizing agent and FeSi75). However, the production of these inputs is accompanied with significant CO_2 emissions (i.e. 3.5 and 4 t CO_2 eq./ton, respectively).

Therefore, adding more steel scrap in the next samples (i.e. IV and V) is associated with a continuous increase in the carbon footprint. However, the carbon footprints of the samples with steel scrap are still lower than sample I. Finally, the mixed alloy (sample VI) has approximately the same carbon footprint as sample V. Despite the low proportion of steel scrap and relinquishing the carburizing agent and FeSi75, the embedded emissions of the pig iron increase the final value. In terms of the costs, sample II also has the best outcome and recorded the lowest costs (approximately 300 EUR/t). Counterintuitively, the alloy with the highest steel scrap (i.e. sample V) has the highest production costs, due to the need to add more expensive additives in order to meet the required specifications.

Herein, it should be highlighted that there are some differences between the conditions in the lab and in industrial facilities that can influence the outcomes slightly. The energy requirement for melting depends, among other things, on the quality of the input materials. For example, clean input materials (i.e. water-, oil- and rust-free) can reduce the combustion as well as the amount of generated slag. A specific energy of approximately 500 kWh/t can be assumed for slagging the sand associated with input materials and a similar consumption can be expected for the rusted materials [53]. For example, if the steel scrap used in alloy V contains 5% impurities, an additional 19 kWh will be required, resulting in approximately 14 kg CO_2 eq. emissions. Herein, it is of particular importance that the scrap used is blasted beforehand to remove any unnecessary residues. Another aspect, which is normally monitored in the laboratory, is the composition of the materials. Knowing the precise compositions of the consumed materials can enable the operator to specify the required charge and electricity input. As a result, the material and energy requirements can be minimized, which means that melting times can be shortened and the operations can be optimized.

Moreover, recovering the waste heat can also decrease the associated carbon emissions. As discussed, the process heat required for the melting process is by far the most energy-intensive process in the foundry industry. Hence, using this heat efficiently afterwards is one of the best ways to achieve CO_2 savings. However, this heat is currently released into the environment as an unused source of energy in many foundries. There are already various examples of how this waste heat can be utilized. For example, the air in the hall and the water in sanitary facilities can be heated with the exhaust air from air compressors [54]. The waste heat can also be used to dry raw and input materials. This process reduces melting times, which in turn reduces the energy requirement. However, the operation times is one of main challenges, as the thermal energy is often only available for a few hours per day when the material is being melted. Hence, storing this heat (e.g. via a heat accumulator) is mandatory in order to be able to use it as an energy source at other times.

Sensitivity Analysis and Validation

As the cutoff approach allocates no emissions to the steel scrap and waste ductile iron, the study conducts a sensitivity analysis in order to illustrate the impact of secondary resources' footprint on the outcomes. Herein, an emission factor of 200 kg CO_2 eq./ton is assumed for the steel scrap and waste ductile iron.[1] Additionally, a sensitivity analysis is conducted for the scrap price, as the price of steel scrap has been increasing in the last years and the figure used in the basic analysis is relatively high compared with the price in 2016 (below 200 EUR/ton) [56]. Therefore, a lower steel scrap price (i.e. 200 EUR/ton) has been considered in the sensitivity analysis to illustrate the relevant impact on costs. The results of both changes are illustrated in Fig. 7. As expected, the carbon footprint has increased with various intensities due to the different steel scrap and pig iron content in the alloys. Although alloy II still has the lowest carbon footprint (i.e. 837 kg CO_2 eq./ton), it recorded the highest increase (i.e. 29.1%). Alloy I also still has the highest carbon footprint (i.e. 1031 kg CO_2 eq./ton), but its relative increase is the lowest (i.e. 18.7%). As can be seen, the impact of the steel scrap price also depends on the alloys' compositions. While the costs of alloy I remains the same, the costs of alloy V decreases 18% to 341.7 EUR/ton, which is the highest relative and absolute decrease.

To validate the environmental and economic analyses, the results have been compared with other studies. The study of [11] reported 300 kg CO_2 eq. for producing 248.5 kg cast iron, which can be converted to approximately 1.2 ton CO_2 eq./ton cast iron. Also, the study of

[1] The value of 200 kg CO_2 eq./ton is used to demonstrate a ratio of the steel's carbon footprint (primary steel 1.9 t CO_2 eq./ton & primary steel 0.4 t CO_2 eq./ton) [55].

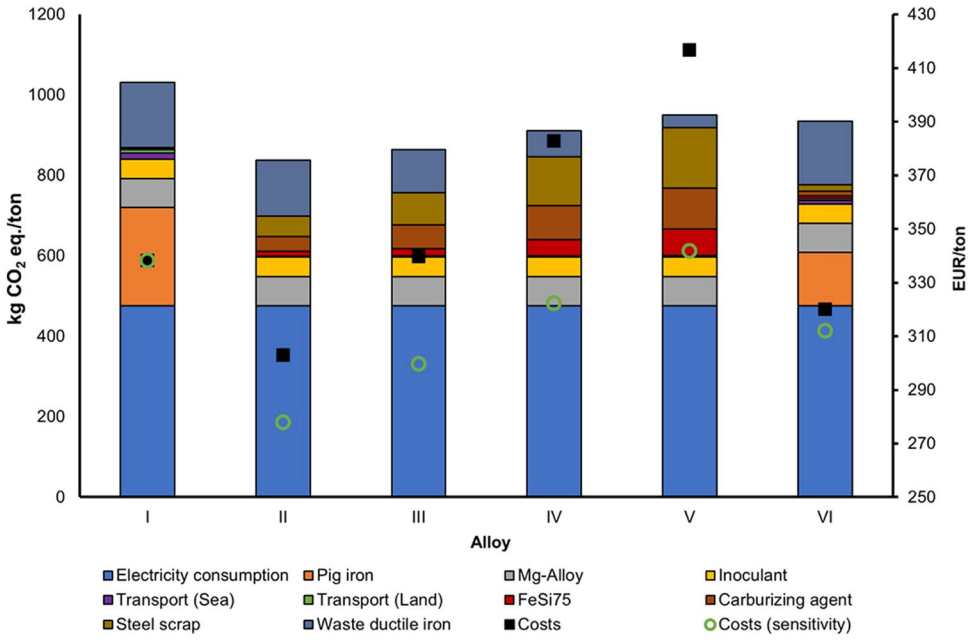

Fig. 7 The sensitivity analysis of the carbon footprint and costs

Table 6 Chemical composition of the investigated alloys (wt%)

Alloy	C	Si	Cr	Mg	Al	Mn	Cu	Fe	CE[a]
II	3.40	2.78 ±0.03	0.004 ±0.003	0.063 ±0.019	0.015 ±0.002	0.207 ±0.002	0.125 ±0.005	Bal.	4.33
III	3.50	2.45 ±0.02	0.056 ±0.000	0.039 ±0.001	0.017 ±0.000	0.247 ±0.003	0.128 ±0.002	Bal.	4.32
IV	3.48	2.43 ±0.03	0.059 ±0.000	0.039 ±0.002	0.014 ±0.000	0.290 ±0.003	0.115 ±0.002	Bal.	4.29
V	3.38	2.56 ±0.02	0.061 ±0.000	0.056 ±0.006	0.016 ±0.001	0.378 ±0.003	0.162 ±0.000	Bal.	4.23

Contents from thermal analysis

[a]CE (carbon equivalent): the CE takes into account the influence of the accompanying elements equivalent to the effect of the carbon and gives a statement about the composition relative to the eutectic composition [CE = C + 1⁄3•Si]

[15] concluded 706 kg CO_2 eq. for manufacturing one ton cast iron. As this study's outcomes range between 650 and 1030 kg CO_2 eq./ton cast iron, the calculated values can be considered reasonable. The deviations between the values can be explained by the different system boundaries, alloy compositions and differing carbon footprints of the inputs. For example, the calculations of [11] used higher emission factors for pig iron and ferrosilicon alloy. For the associated costs, the average ductile cast iron price at the factory gate in NRW is 1437.5 EUR/t [57]. In addition, according to [58], the materials and energy inputs contribute to 40% of the final costs. Therefore, the calculated costs of the investigated flows should be reasonable (277–417 EUR/t) as the calculations did not include some materials such molding and energy inputs such as warmth maintenance.

Technical Performance

In order to make sure that the alloys fulfill the standard requirements when steel scrap and additives are used, alloys II–V were produced and studied with regard to their chemical composition and microstructural and mechanical properties.

Chemical Composition

All alloys were produced and casted in accordance with ductile iron grade EN-GJS-400-15 (DIN EN 1563). Hence, a targeted carbon content of 3.4 wt% and silicon content of 2.5 wt% was set for each alloy. However, for producing the alloys, different contents of steel scrap and recycled material

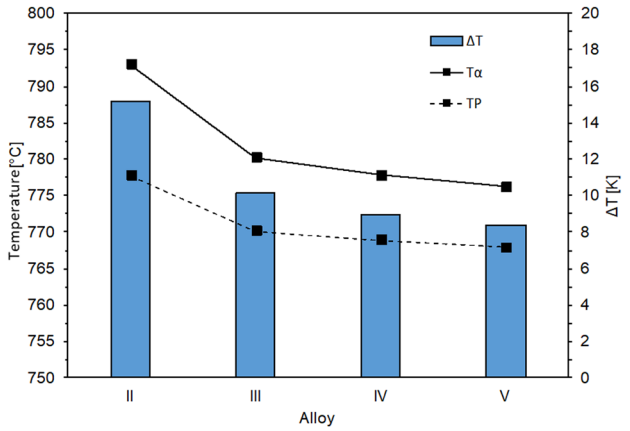

Fig. 8 Effect of steel scrap content on T_α, T_p and ΔT

were used according to Fig. 2. As indicated in Table 6, the carbon and silicon contents could be held quite constant by setting different amounts of steel scrap and recycled material. Furthermore, the magnesium, aluminum and copper contents remain constant regardless of the selected composition of the charging. The variations of the residual magnesium content between the individual alloys of approximately 0.02 wt% are considered to be process-dependent. However, it can be noted that the chromium and manganese content exhibit a significant increase due to the growth of the steel scrap content from 25 wt% in alloy II to 75 wt% in alloy V. Above steel scrap contents of 40 wt%, significant Cr contents of 0.056 wt% occur. The Mn content, on the other hand, increases continuously with increasing steel scrap content up to 0.378 wt% in alloy V.

Based on the chemical compositions that have been shown, ferrite and pearlite formation temperatures T_α and T_p and the eutectoid temperature interval were calculated according to [59], indicated in Eqs. 1–3.[2] The results of these calculations are shown in Fig. 8. It can be observed that the stable eutectoid temperature decreases significantly more than the metastable eutectoid temperature with increasing steel scrap content. This leads to a reduction of the eutectoid temperature interval with increasing steel scrap content in the alloy. The reason for this is the increased content of pearlite-stabilizing elements, including in particular Cr and Mn. Due to the reduction of ΔT, an increased pearlite content has to be expected in the corresponding alloys. In order to verify this hypothesis, microstructural analyses were further carried out with the aim of quantifying the respective phase fractions of the alloy (graphite, matrix phase).

$$T_\alpha = 739 + 18.4\mathrm{Si} + 2\mathrm{Si}^2 - 14\mathrm{Cu} - 45\mathrm{Mn} + 2\mathrm{Mo} - 24\mathrm{Cr} - 27.5\mathrm{Ni} \quad (1)$$

$$T_p = 727 + 21.6\mathrm{Si} + 0.023\mathrm{Si}^2 - 21\mathrm{Cu} - 25\mathrm{Mn} + 8\mathrm{Mo} + 13\mathrm{Cr} - 33\mathrm{Ni} \quad (2)$$

$$\Delta T = 12 - 3.2\mathrm{Si} + 1.977\mathrm{Si}^2 + 7\mathrm{Cu} - 20\mathrm{Mn} - 6\mathrm{Mo} - 37\mathrm{Cr} + 5.5\mathrm{Ni} \quad (3)$$

Microstructure

Figure 9 shows representative microstructural images for the study after Nital-etching of alloys II–V, arranged in order of increasing steel scrap content from top to bottom and increasing thermal modulus from left to right. With higher steel scrap content, an increasing pearlite content can be observed. All of the produced alloys show significant pearlite fractions from about 25 to 50%. This confirms the previously assumed difficulties associated with the use of steel scrap or the accompanying elements contained within it.

Herein, there is an overlapping of different effects. On the one hand, less pearlite is generated at larger moduli. On the other hand, a higher graphite nodule count leads to shorter carbon diffusion paths. As a result, ferrite formation instead of pearlite formation is promoted in these areas. Furthermore, there is a clear trend indicating higher pearlite contents with increasing thermal modulus, as confirmed by Fig. 10. At low thermal modulus, higher undercooling occurs and therefore a higher nodule count is generated leading to shorter diffusion paths for carbons during further solidification and cooling. Therefore, carbon atoms must diffuse to existing graphite precipitates in a shorter time range. A lower carbon diffusion time leads to a higher roundness of graphite particles and a higher nodularity of the sample. Figure 11 summarizes the effect of different steel scrap additions on both the pearlite fraction in the microstructure and the eutectoid transformation interval.

Figure 12 shows the results of the graphite analysis using automatic image evaluation. In the four-test series, there is no noticeable difference with regard to nodularity. Comparing a casting modulus of 0.8 cm with a higher wall thickness, it is noticed that the thinner components have a higher nodularity in most cases, which is corresponding to the literature [9, 60]. The nodularity of the 0.8 cm module is on average 70%. In contrast, the average nodularity of the larger wall thicknesses is 49%. The count of graphite nodule decreases with increasing thermal modulus. For a casting modulus of 3.29 cm, the average nodule count is 73 1/mm^2. In contrast, the casting modulus of 0.8 cm exhibits a nodule count of 179 1/mm^2 on average (+105 1/mm^2).

[2] Element contents in wt%

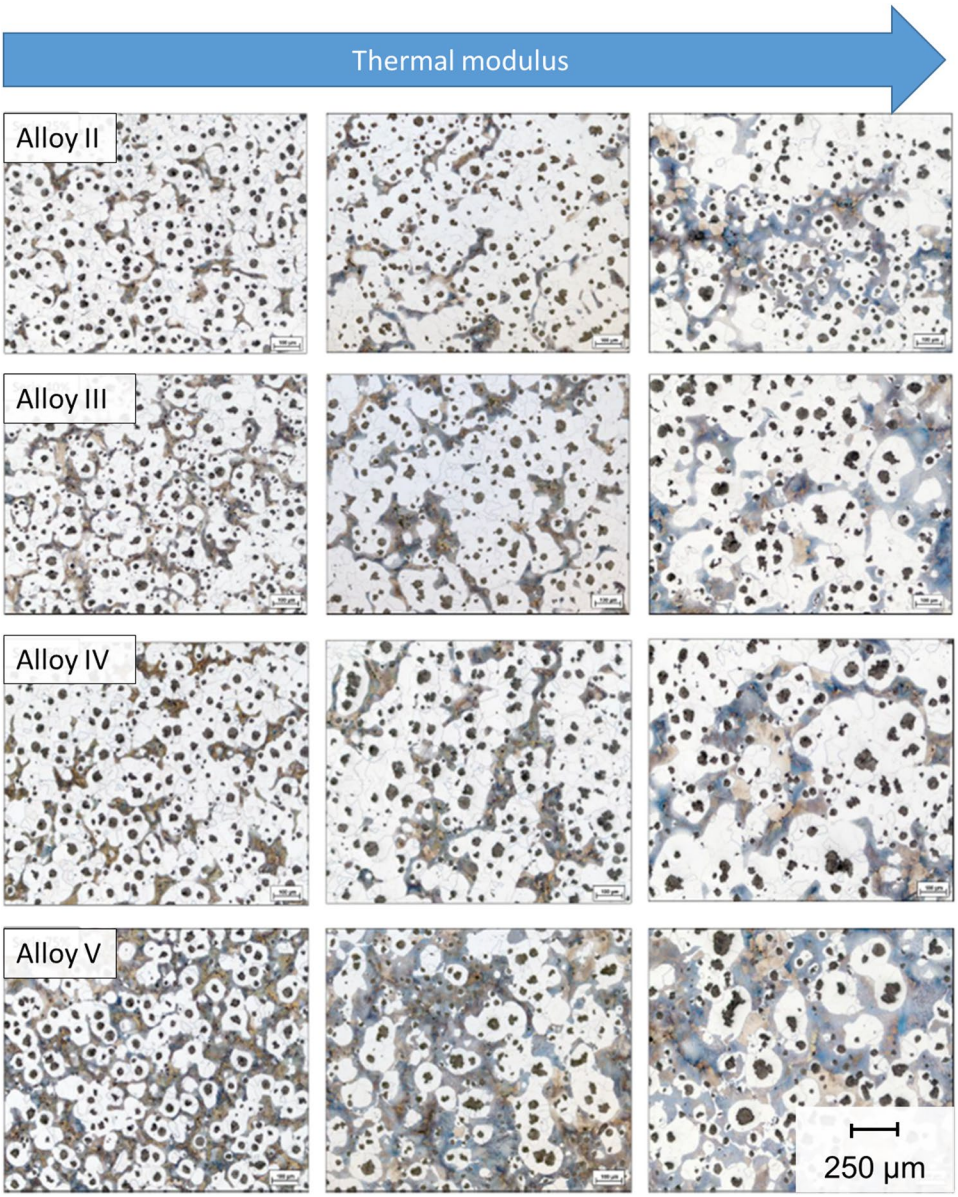

Fig. 9 Microstructure of the investigated alloys (nital-etched specimens at ×100 magnification) [recognizable are graphite nodules (black), ferrite (white) and perlite (colored)] (Color figure online)

Mechanical Properties

As shown in Fig. 13, the minimum requirement for tensile strength (UTS = 400 MPa for a wall thickness of up to 30 mm according to DIN EN 1563) has been achieved in all adjusted alloys. In some cases, the strengths are well above 500 MPa. The UTS increase significantly with increasing the steel scrap content. For example, it exhibits a UTS of 490 MPa at a steel scrap content of 25% and 610 MPa at a content of 75% steel scrap. A significant correlation between the pearlite fraction in the microstructure and the UTS can be observed from Fig. 14. The influence of the modulus on the strength is reflected in a decrease in strength; this applies across the board to all steel scrap contents. The standard specifies a yield strength of 250 MPa for the material EN-GJS-400–15. This value was exceeded in all samples, as indicated in Fig. 15. The same trend as for the tensile strength can be observed, with similar or slightly decreasing values from 25 to 60 wt% steel scrap content. Alloy V shows a strongly increased yield strength. The desired elongation at fracture of 15% could be achieved in specimens with moduli of 0.96 and 1.74 cm up to a content of 60 wt% steel scrap (see Fig. 16). It can be noted that the elongation at fracture of the cylindrical specimens of up to 5.5% is significantly lower. When 75 wt% steel scrap is used in alloy V, no sufficient elongation at fracture was found in any of the cases investigated, so this alloy does not meet the requirements of EN-GJS-400-15 and cannot be used. This observation is attributed to the higher amount of pearlite- and carbide-stabilizing elements that are added to the melt due to higher

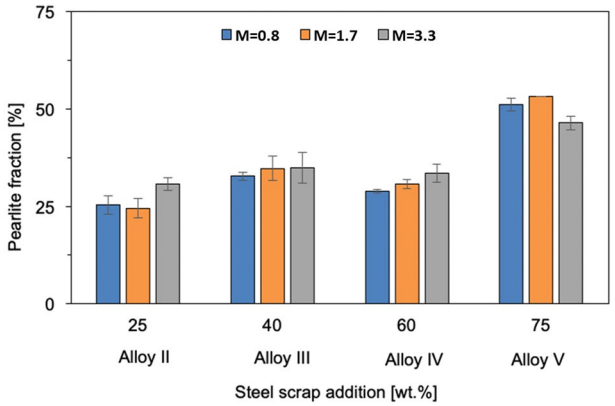

Fig. 10 Amount of pearlite fraction in the steel alloys as a function of steel scrap addition and thermal modulus (M) of the different casting geometries

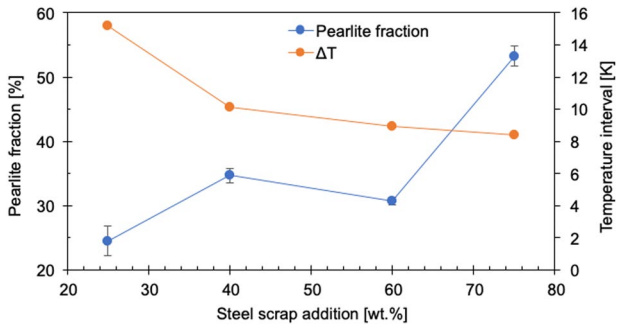

Fig. 11 Effect of steel scrap addition on the pearlite fraction and eutectoid temperature interval

amounts of steel scrap. Maximum amounts of Mn in alloy V and a pearlite content of 52% in the microstructure confirm these results, as they are acting as crack initiation sites during the mechanical testing of the alloys.

Conclusions and Outlook

The analyses have clearly depicted the correlation between the technical, economic and environmental aspects of the cast iron production. The environmental analyses show that the addition of steel scrap up to a content of 60 wt% results in significant CO_2 savings compared to an alloy with 15 wt% pig iron and no steel scrap. Therefore, using steel scrap is superior from an environmental perspective. However, exceeding a certain threshold (i.e. 25 wt%) can lead to a relapse due to the ferrosilicon and carbon that have to be added (to yield comparable composition and technical performance), which have high embedded carbon emissions. For the investigated alloys, the use of steel scrap is recommended with a content between 25 and 40 wt% with lower

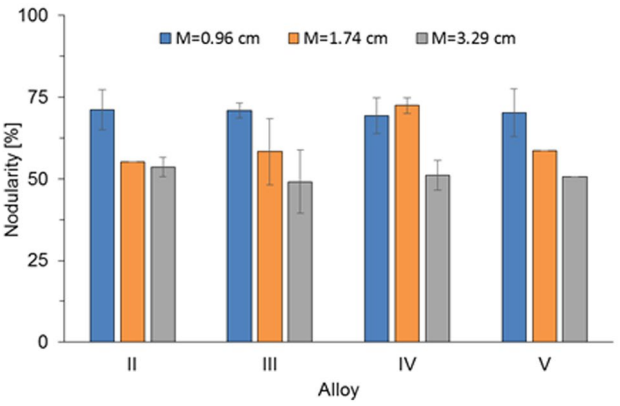

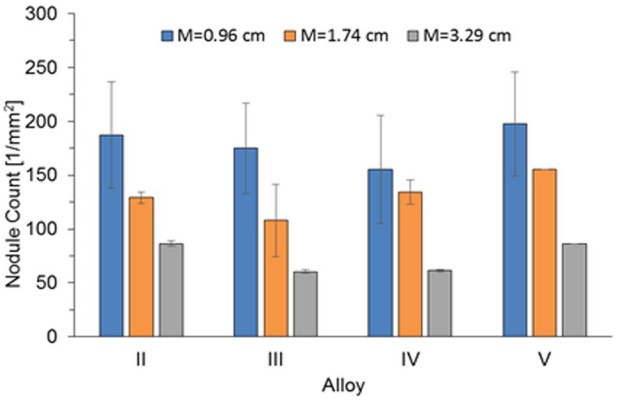

Fig. 12 Nodularity and graphite nodule count of the investigated alloys

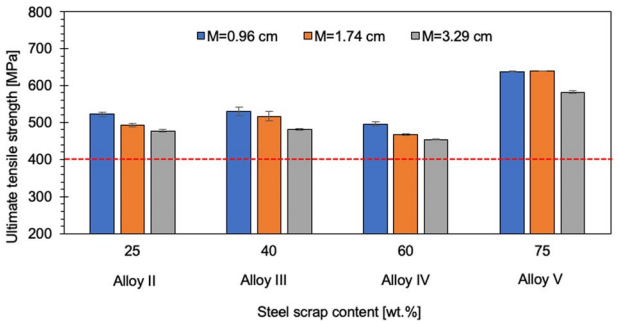

Fig. 13 Ultimate tensile strength of the investigated alloys (the red line is the minimum strength threshold to meet alloy specification) (Color figure online)

emissions of 25 wt%. A comparable result could be taken from the cost calculations; the costs also increase with the steel scrap content due to the required expensive additives such as ferrosilicon and carburizing agents. The results of this study show that the use of steel scrap is only profitable up to just under 40 wt% from an economic point of view.

Similar conclusions can be also drawn from the results of the experimental tests. It can be seen that the mechanical

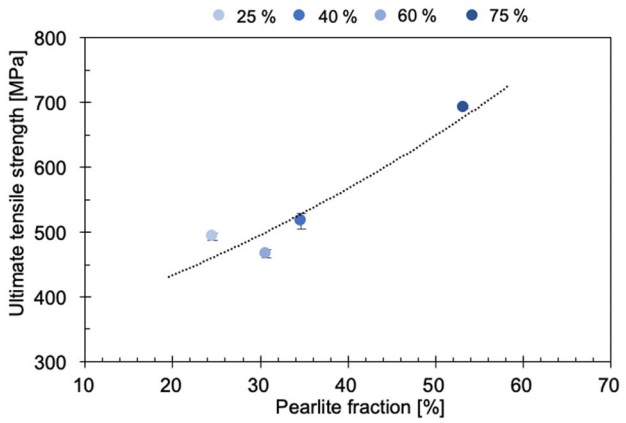

Fig. 14 Effect of pearlite fraction on UTS for different amounts of steel scrap

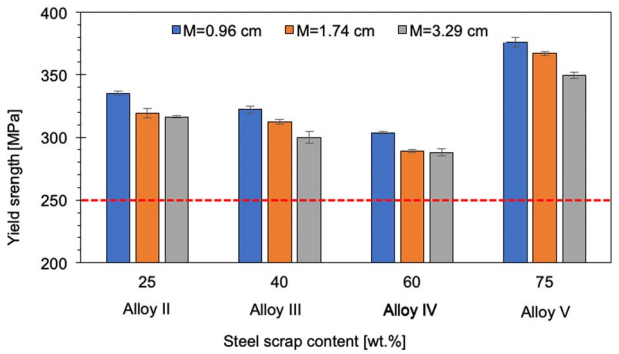

Fig. 15 Influence of steel scrap addition on the yield strength of alloy II–V (the red line is the minimum strength threshold to meet alloy specification) (Color figure online)

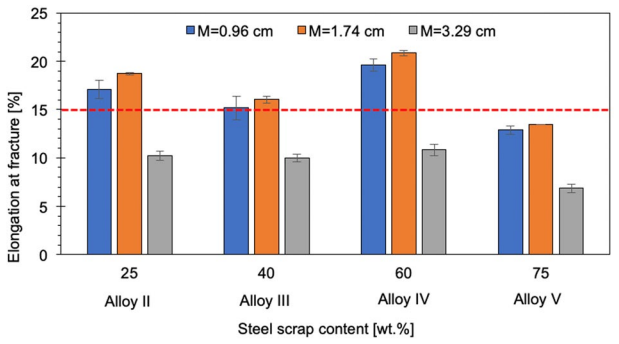

Fig. 16 Effect of the steel scrap content on the elongation at fracture of the investigated alloys (the red line is the minimum strength threshold to meet alloy specification) (Color figure online)

properties according to DIN EN 1563 could be safely achieved or slightly exceeded at low moduli for all investigated alloys. However, the required elongation at fracture could not be achieved in alloy V with an addition of 75 wt% steel scrap due to the increased pearlite content in the microstructure. The reason for this is the elevated content of pearlite-stabilizing elements, in particular Mn, that originate from the steel scrap. Comparing the different results, it becomes apparent that the use of steel scrap up to a proportion of 60 wt% can be recommended from a technical and metallurgical perspective, as both the UTS, YS and elongation at fracture are met according to the technical requirements (UTS = 400 MPa, YS = 250 MPa, $A = 15\%$ for wall thicknesses lower than 30 mm). However, the limiting factor is the wall thickness which lowers the mechanical properties generally. However, the elongation at fracture remains the critical factor, as it decreases due to the increased pearlite content as a result of the higher steel scrap contents. For a steel scrap content of 75 wt%, an elongation at fracture of only 12.9% is achieved in a wall thickness of 25 mm.

Apart from the input materials, energy consumption is generally responsible for the largest proportion of the carbon footprint. Therefore, minimizing the energy requirements and recovering the waste heat can lead to lower GHG emissions. Herein, the existing practices in the foundries should be further investigated and available efficiency measures have to be adopted. Moreover, shifting the electricity mix towards more renewable energies should result in a carbon–neutral melting process. Herein, eliminating the fossil-based technologies such copula furnace and increasing the share of electricity-based ones such as induction furnaces are also crucial. Similarly, adopting more climate-neutral production processes for the other material inputs can reduce the embedded emissions such as employing iron reduced via hydrogen or using biogenic carbon and carbon capture and storage (CCS) while producing the other inputs.

The framework presents a scientific frame by which the technical, economic and environmental impacts can be investigated and optimized. The main advantage of the presented method is the possibility to be adopted easily by the foundries. It is a very cost-effective approach as it does not need innovative technologies with high capital costs such as furnaces. However, the study is still introductory and further analyses have to be performed. As increasing the steel scrap consumption by the cast industry can influence the supply in the steel industry, intersectoral analyses will be needed to determine where steel scrap should be used to achieve the best environmental impact. Also, the analyses focus on a specific type of cast iron and certain alloys. Therefore, further alloys and metals have to be investigated.

The industry should consider all the CO_2-intensive processes in foundries. Due to the variety of the casting technologies and the large number of products, a "one-solution-fits-all" approach will be ineffective. Hence, more investigations and better classification are needed in order to derive diverse mitigation strategies that can suit a wide-range of the producers. Conducting such investigations and

adopting sophisticated measures also necessitates systematization and acquiring all energy-related data in the foundries. Therefore, establishing energy management systems is also mandatory in order to improve the energy use continuously and achieve the planned energy savings.

There are some limitations and uncertainties of the presented outcomes. First, although the study strived for considering actual industrial parameters such as prices and emission factors, these values may not be the same for all producers, especially in other regions. Second, some laboratory practices may not be adopted in the foundries and vice versa, such as scrap cleaning. Third, the study used a certain type of the melting furnace, while the foundries may use other furnaces with different efficiencies and energy consumption. Fourth, the study adopted a cutoff approach and scenario analysis for the carbon footprint of secondary inputs. Hence, using another allocation approach can result in different outcomes and conclusions. Therefore, additional studies are needed to compare allocation methods in order to derive an agreed-upon approach. Moreover, the environmental analysis focused exclusively on determining the carbon footprint of different alloys. Therefore, integrating more environmental impact categories could provide more insights and conclusions.

Acknowledgements This study was financed by SCI4climate.NRW project (funded by the ministry of economic affairs, innovation, digitalization and energy of the state of North Rhine-Westphalia) [61]. The authors would like to thank the editor and reviewers for their insightful comments and valuable suggestions for improving the manuscript. The authors also gratefully acknowledge the provision of data by Foundry J. D. Brackelsberg GmbH [47]. Further thanks go to Ingo Braun for supporting the experimental casting trials, Stefanie Düker for assisting the metallographic analysis and Claus Groten for the mechanical testing of the alloys.

Funding Open Access funding enabled and organized by Projekt DEAL.

Declarations

Conflict of interest The authors declare that they have no conflict of interest.

References

1. BMU (2021) Lesefassung des Bundes-Klimaschutzgesetzes 2021 mit markierten Änderungen zur Fassung von 2019 (Bundesministerium für Umwelt, Naturschutz und nukleare Sicherheit (BMU))
2. UBA (2020) Jährliche Treibhausgas-Emissionen in Deutschland/Annual greenhouse gas emissions in Germany. Umweltbundesamt (UBA)
3. Labrecque C, Cabanne PM, Muratore EC (2011) Kaltzähigkeit von Gusseisen mit Kugelgraphit für Windenergieanlagen. Giesserei-Praxis 9(2011):430–438
4. Mikoleizik P, Geier G (2014) SiWind—Werkstoffentwicklung für Offshore-Windenergieanlagen im Multi-Megawatt-Bereich. Giesserei 101(09):64–69
5. Khan MAA, Sheikh AK, Al-Shaer BS (2017) Evolution of metal casting technologies—a historical perspective. Springer, Cham. https://doi.org/10.1007/978-3-319-46633-0_1
6. BDGUSS (2021) Die Gießerei-Industrie in Deutschland (Der Bundesverband der Deutschen Gießerei-Industrie e. V.)
7. Lickfett H, Sand TVD (2021) Perspektive 2021/22—Gießerei-Industrie im Umbruch (bdguss)
8. CAEF (2021) The European foundary industry 2020—Annual statistics and national reports. The European Foundary Association (CAEF)
9. Stefanescu DM (2017) ASM handbook: cast iron science and technology, vol 1A, ASM International
10. Kotzin EL (2002) Timeline of casting technology. American Foundry Society. https://www.thefreelibrary.com/Timeline+of+casting+technology%3A+with+a+history+set+in+motion+before…-a095355710. Accessed 24 July 2022
11. Jhaveri K, Lewis GM, Sullivan JL et al (2018) Life cycle assessment of thin-wall ductile cast iron for automotive lightweighting applications. Sustain Mater Technol 15:1–8. https://doi.org/10.1016/j.susmat.2018.01.002
12. Salonitis K, Jolly M, Pagone E et al (2019) Life-cycle and energy assessment of automotive component manufacturing: the dilemma between aluminum and cast iron. Energies 12(13):2557. https://doi.org/10.3390/en12132557
13. Recio JMB, Guerrero PJ, Ageitos MG, et al (2005) Estimate of energy consumption and CO2 emission associated with the production, use and final disposal of PVC, HDPE, PP, ductile iron and concrete pipes. Report: PVC-Tub-200512-2 (Environmental Modelling Laboratory—Department de Projectes d'Enginyeria—Universitat Politecnica de Catalunya)
14. Chilana L, Bhatt AH, Najafi M et al (2016) Comparison of carbon footprints of steel versus concrete pipelines for water transmission. J Air Waste Manage Assoc 66(5):518–527. https://doi.org/10.1080/10962247.2016.1154487
15. Joshi D, Modi Y, Ravi B (2011) Evaluating environmental impacts of sand cast products using life cycle assessment. In: ICORD 11: proceedings of the 3rd international conference on research into design engineering (section: eco-design, sustainable manufacturing, design for sustainbility), Bangalore, India, 10.-12.01.2011, pp 551–558. (www.designsociety.org)
16. Mitterpach J, Hroncová E, Ladomerský J et al (2017) Environmental evaluation of grey cast iron via life cycle assessment. J Clean Prod 148:324–335. https://doi.org/10.1016/j.jclepro.2017.02.023
17. Zheng J, Huang B, Zhou X (2018) A low carbon process design method of sand casting based on process design parameters. J Clean Prod 197:1408–1422. https://doi.org/10.1016/j.jclepro.2018.06.285
18. Neumann F, Reuter MA (2021) Simulationsbasierte Berechnung der Umweltwirkung von Zinkdruckguss bei Einsatz von Primär- und Sekundärrohstoffen für die Legierungsherstellung—Initiative ZINK (Redaktioneller Beitrag). https://www.zink.de/wp-content/

uploads/2021-11_Sim-Berechnung-LCA-Sekund%C3%A4rzink_ZnD_final.pdf. Accessed 24 July 2022
19. Energie Innovation Austria (EI) (2013) Energieeffizienz in der Industrie Innovation am Produktionsstandort Österreich. CO_2-minimierte Roheisenproduktion mit vorreduzierten Eisenträgern. Bundesministerium für Verkehr, Innovation und Technologie, Austria
20. DIN (2019) DIN EN ISO 945-1: Gießereiwesen—Gusseisen mit Kugelgraphit; Deutsche Fassung EN 1563:2018 (Deutsches Institut Für Normung e.V.)
21. Menk W (2018) A new high strength high ductile nodular iron. Mater Sci Forum 925:224–230. https://doi.org/10.4028/www.scientific.net/MSF.925.224
22. Magnusson Åberg L, Hartung C (2012) Solidification of SiMo nodular cast iron for high temperature applications. Trans Indian Inst Met 65(6):633–636. https://doi.org/10.1007/s12666-012-0216-8
23. Madias J (2010) Alternatives for hot metal production: Cupola, induction and arc furnace. In: COLFUN conference, Buenos Aires, Argentina, 28–30 October 2010
24. Zhu X, Jin Q, Ye Z (2020) Life cycle environmental and economic assessment of alumina recovery from secondary aluminum dross in China. J Clean Prod 277:123291. https://doi.org/10.1016/j.jclepro.2020.123291
25. Zhu X, Jin Q (2021) Comparison of three emerging dross recovery processes in chinas aluminum industry from the perspective of life cycle assessment. ACS Sustain Chem Eng 9(19):6776–6787. https://doi.org/10.1021/acssuschemeng.1c00960.s001
26. Volk R, Stallkamp C, Steins JJ et al (2021) Techno-economic assessment and comparison of different plastic recycling pathways: a German case study. J Ind Ecol 25(5):1318–1337. https://doi.org/10.1111/jiec.13145
27. Singh A, Rorrer NA, Nicholson SR et al (2021) Techno-economic, life-cycle, and socioeconomic impact analysis of enzymatic recycling of poly(ethylene terephthalate). Joule 5(9):2479–2503. https://doi.org/10.1016/j.joule.2021.06.015
28. Bora RR, Wang R, You F (2020) Waste polypropylene plastic recycling toward climate change mitigation and circular economy: energy, environmental, and technoeconomic perspectives. ACS Sustain Chem Eng 8(43):16350–16363. https://doi.org/10.1021/acssuschemeng.0c06311.s001
29. Voss R, Lee RP, Fröhling M (2022) Chemical recycling of plastic waste: comparative evaluation of environmental and economic performances of gasification- and incineration-based treatment for lightweight packaging waste. Circ Econ Sustain. https://doi.org/10.1007/s43615-021-00145-7
30. DIN (2019) DIN EN ISO 14067:2019-02. Treibhausgase—Carbon Footprint von Produkten—Anforderungen an und Leitlinien für Quantifizierung (ISO 14067:2018); Deutsche und Englische Fassung EN ISO 14067:2018 (Deutsches Institut Für Normung e.V.). https://doi.org/10.31030/2851769
31. Ecoinvent. Ecoinvent database 3.5 2018
32. US EPA (2009) Technical Support document for the ferroalloy production sector: proposed rule for mandatory reporting of greenhouse gases. In: Office of air and radiation (U.S. Environmental Protection Agency)
33. Monsen BE, Lindstad T, Tuset JK (1998) CO_2 emissions from the production of ferrosilicon and silicon metal in Norway. In: 1998 electric furnace conference proceedings
34. ASK Chemicals (2017) Metallurgie—produktlinienüberblick. https://www.ask-chemicals.com/fileadmin/user_upload/Download_page/foundry_products_brochures/DE/Metallurgy_Overview_DE.pdf. Accessed 24 July 2022
35. Dötsch E (2019) Induktives Schmelzen und Warmhalten. Grundlagen—Anlagenaufbau—Verfahrenstechnik, 3. Auflage. Prozesswärme Edition, Vulkan Verlag, Essen
36. Allacker K, Mathieux F, Pennington D et al (2017) The search for an appropriate end-of-life formula for the purpose of the European Commission Environmental Footprint initiative. Int J Life Cycle Assess 22(9):1441–1458. https://doi.org/10.1007/s11367-016-1244-0
37. Nicholson AL, Olivetti EA, Gregory JR, et al (2009) End-of-life LCA allocation methods: open loop recycling impacts on robustness of material selection decisions. In: 2009 IEEE international symposium on sustainable systems and technology, pp 1–6. https://doi.org/10.1109/ISSST.2009.5156769
38. WSA (2015) Steel in the circular economy: a life cycle perspective. World Steel Association (WSA); Brussels 2015. https://worldsteel.org/publications/bookshop/circular-economy-life-cycle-steel/. Accessed 24 July 2022
39. Dubreuil A, Young SB, Atherton J et al (2010) Metals recycling maps and allocation procedures in life cycle assessment. Int J Life Cycle Assess 15(6):621–634. https://doi.org/10.1007/s11367-010-0174-5
40. Frees N (2008) Crediting aluminium recycling in LCA by demand or by disposal. Int J Life Cycle Assess. https://doi.org/10.1065/lca2007.06.348
41. Santero N, Hendry J (2016) Harmonization of LCA methodologies for the metal and mining industry. Int J Life Cycle Assess 21(11):1543–1553. https://doi.org/10.1007/s11367-015-1022-4
42. Rehberger M, Hiete M (2020) Allocation of environmental impacts in circular and cascade use of resources—incentive-driven allocation as a prerequisite for cascade persistence. Sustainability 12(11):4366. https://doi.org/10.3390/su12114366
43. Norgate T (2013) Metal recycling: the need for a life cycle approach. EP135565, CSIRO, Australia. https://publications.csiro.au/rpr/download?pid=csiro:EP135565&dsid=DS2. Accessed 24 July 2022
44. Backes JG, Suer J, Pauliks N et al (2021) Life cycle assessment of an integrated steel mill using primary manufacturing data: actual environmental profile. Sustainability 13(6):3443. https://doi.org/10.3390/su13063443
45. OpenLCA. OpenLCA 1.10.3 2021
46. Bundesnetzagentur (2022) Pressemitteilung: Bundesnetzagentur veröffentlicht Daten zum Strommarkt 2021
47. Brackelsberg (2022) Data from J.D. Brackelsberg GmbH
48. DIN (2019) DIN EN 1563: Gießereiwesen—Gusseisen mit Kugelgraphit; Deutsche Fassung EN 1563:2018 (Deutsches Institut Für Normung e.V.)
49. Riebisch MF (2021) Erarbeitung eines Prozessfensters zur Vermeidung unterkühlungs- und seigerungsbedingter Karbide in hochsiliziumhaltigem Gusseisen mit Kugelgraphit: RWTH Aachen University. https://doi.org/10.18154/RWTH-2021-04073
50. DIN (2009) DIN EN ISO 6892-1: metallische Werkstoffe—Zugversuch—Teil 1: Prüfverfahren bei Raumtemperatur (ISO 6892-1:2009). Deutsche Fassung EN ISO 6892-1:2009, ICS 77.040.20. (Deutsches Institut Für Normung e.V.)
51. ISO (2019) ISO/FDIS 945–4: microstructure of cast irons—Part 4: test method for evaluation nodularity in spheroidal graphite cast irons (International Organization for Standarization)
52. Riebisch M (2021) Erarbeitung eines Prozessfensters zur Vermeidung unterkühlungs- und seigerungsbedingter Karbide in hochsiliziumhaltigem Gusseisen mit Kugelgraphit
53. Bosse M (2013) Energieeffiziente Gattierung und Einfluss der Chargenzusammensetzung auf die Energieeffizienz. Energieeffizienter Gießereibetrieb 2.0 (BDGUSS)
54. Bosse M (2016) Abwärmeverstromung muss sich wieder lohnen! GIESSEREI 103 (Ausgabe 06/2016)

55. Material Economics (2019) Industrial transformation 2050—pathways to net-zero emissions from EU Heavy Industry
56. BDSV (2016) BDSV Durchschnittliche Lagerverkaufspreise für bestimmte Stahlschrottsorten in Deutschland—2016—Bundesweit. Bundesvereinigung Deutscher Stahlrecycling- und Entsorgungsunternehmen e. V. (BDSV)
57. IT NRW (2022) Vierteljährliche Produktionserh. im Verarb. Gewerbe: Wert, Betriebe der zum Absatz bestimmten Produktion nach dem Güterverzeichnis 2019 (9-Steller) - Land - Jahr (GP2019 = 245112900 & Year = 2019). Statistisches Landesamt—Information und Technik Nordrhein-Westfalen. https://www.landesdatenbank.nrw.de/ldbnrw//online?operation=table&code=42131-03i&bypass=true&levelindex=1&levelid=1658746667613#abreadcrumb. Accessed 24 July 2022
58. Haidar S, Sekh M, Islam A et al (2019) Best practices in ductile iron foundries to increase productivity and profitability. Indian Foundry Congress, Delhi
59. Lacaze J, Sertucha J, Åberg LM (2016) Microstructure of as-cast ferritic-pearlitic nodular cast irons. ISIJ Int 56(9):1606–1615. https://doi.org/10.2355/isijinternational.ISIJINT-2016-108
60. Borrajo JM, Martínez RA, Boeri RE et al (2002) Shape and count of free graphite particles in thin wall ductile iron castings. ISIJ Int 42(3):257–263. https://doi.org/10.2355/isijinternational.42.257
61. SCI4climate.NRW (2021) SCI4climate.NRW project. https://www.in4climate.nrw/en/stakeholders/scientific-community. Accessed 24 June 2021